JOC The Journal of Organic Chemistry

Article

pubs.acs.org/joc

Theoretical Study of the Importance of the Spectator Groups on the Hydrolysis of Phosphate Triesters

José R. Mora,[†] Anthony J. Kirby,*[,‡] and Faruk Nome*[,†]

[†]Department of Chemistry, National Institute of Catalysis, Federal University of Santa Catarina, Florianópolis, Santa Catarina 88040-900, Brazil

[‡]University Chemical Laboratory, University of Cambridge, Cambridge CB2 1EW, U.K.

Supporting Information

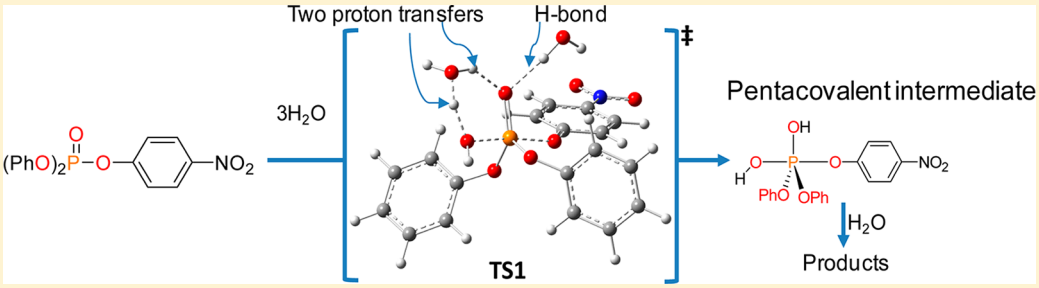

ABSTRACT: The spontaneous hydrolysis of a series of five triaryl and two dialkyl aryl phosphate triesters, previously studied experimentally, is examined theoretically using two different hybrid density functional methods, B3LYP and M06; two basic sets, 6-31+G(d) and 6-311++G(d,p); and the Gaussian 09 program. The B3LYP/6-31+G(d) methodology combined excellent accuracy with minor computational cost. The calculations show excellent quantitative agreement with experiment, which is best in the presence of three discrete water molecules. The results support a two-step mechanism involving a pentacovalent addition intermediate, with a lifetime of tenths of a millisecond. The rate-determining formation of this intermediate involves general base catalysis, defined by concerted proton transfers in a six-membered cyclic activated complex (**TS1**), which involves two hydrogen-bonded water molecules supporting a well-developed $H_2O\cdots P$ bond (mean % evolution 77.83 ± 0.97). The third water molecule is hydrogen-bonded to P═O and subsequently involved in product formation via **TS2**. The effects on reactivity of all the groups attached to phosphorus in **TS1** are examined in detail: the two non-leaving groups in particular are found to play an important role, accounting for the substantial difference in reactivity between triaryl and dialkyl aryl phosphate triesters.

INTRODUCTION

Phosphate esters play important roles in many areas of science. Mono- and diesters are involved in countless biological processes, most prominently the storage and transmission of genetic information involving DNA and RNA. Our current understanding of their chemistry is derived from many years of mechanistic work on simple systems. The evidence is summarized and discussed in detail in excellent recent reviews.[1−3]

Triesters do not occur naturally, but together with related compounds have found widespread use as herbicides and insecticides since the mid-20th century. Their powerful anticholinesterase activities led to the further development of a range of nerve gas agents and the consequent drive for efficient antidotes to organophosphorus poisons. Nature's response, mirroring the appearance of β-lactamases set in train by the mass use of β-lactam antibiotics, has been the evolution of new phosphotriesterase enzymes.[4] The community's response lies in the strong current interest in the development of catalysts[5,6] or other means capable of destroying stockpiles of these deadly agents safely and economically.[7,8] These developments emphasize the need for a better understanding of the intrinsic reactivity of phosphate triesters, as non-natural substrates in biological systems and as well-defined but little studied organic systems.

Early work followed the investigations of the hydrolysis of mono- and diesters in concentrating on the dependence of reactivity on the nucleophile and the leaving group. α-Effect nucleophiles[9] such as hydroxylamine and the hydroperoxide anion show exceptionally high activity toward phosphorus triesters, and a good leaving group is key to the high activity of organophosphorus poisons.[10] However, recent experimental work on triester reactivity has suggested an unexpectedly strong dependence on the non-leaving groups RO in the spontaneous hydrolysis reaction (Scheme 1).[11]

Scheme 1. Spontaneous Hydrolysis Reaction of Triesters

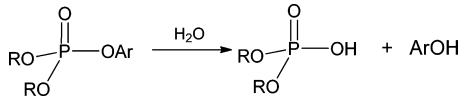

Received: July 2, 2012
Published: July 26, 2012

   dx.doi.org/10.1021/jo301380v | J. Org. Chem. 2012, 77, 7061−7070

Scheme 2. Concerted (a) and Stepwise (b) Mechanisms for the Alkaline Hydrolysis of Dimethyl Phosphate Triesters

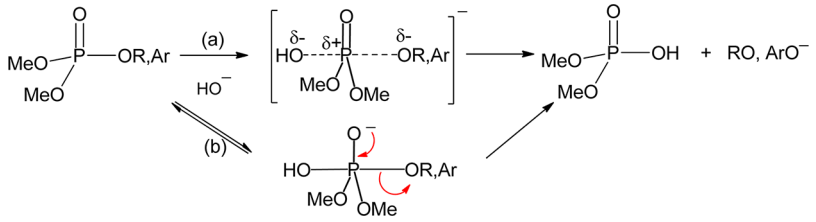

Scheme 3. Triaryl and Dialkyl Aryl Phosphate Triesters Used in This Work

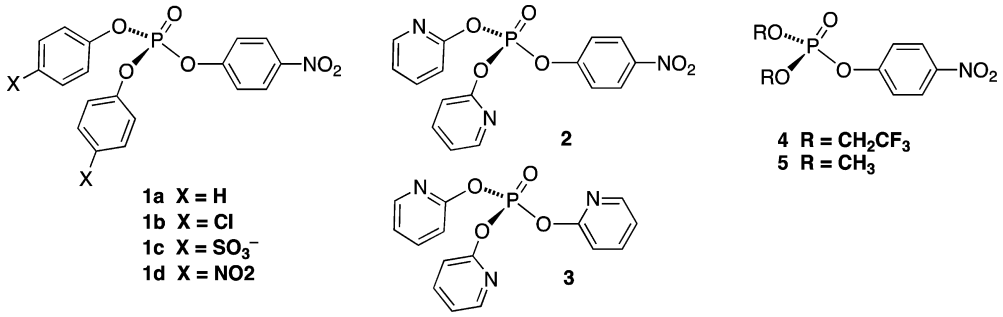

Theoretical work has also concentrated on the reactions of mono- and diesters.[12−15] Recent calculations on triesters have examined the hydrolysis of the pesticide ethyl paraoxon (diethyl 4-nitrophenyl phosphate),[16] and of its dimethyl ester analogue methyl paraoxon[17] catalyzed by the binuclear zinc enzyme phosphotriesterase (PTE). The enzyme uses a zinc-bound hydroxide as the nucleophile. Zhang et al. used QM(PM3)/MM molecular dynamics simulations combined with QM(DFT)/MM optimizations to arrive at a mechanism in which nucleophile, phosphorus center, and the oxygen of the leaving group are positioned in the linear orientation expected for an $S_N2(P)$ reaction, which proceeds by way of a short-lived pentacoordinate intermediate. The calculations of Chen et al. used density functional theory (DFT) with the functional B3LYP, performed without MD simulation and with geometry optimization using a 6-31G(d,p) basis set for C, H, O, N, and P and a LANL2DZ basis set for Zn. This work reported strong support for a stepwise mechanism, also involving a short-lived pentacoordinate intermediate with the first step being rate-determining.

Recent theoretical work using the hybrid functional B3LYP evaluated the effect of varying the leaving group on the alkaline hydrolysis mechanism for six different dimethyl phosphate triesters.[18] Concerted and stepwise mechanisms (Scheme 2) were considered, and the results suggested a change from a stepwise mechanism for reactions of esters with poor leaving groups ($pK_{LG} > 8$) to a concerted reaction for esters with good leaving groups.

Our recent results on the (much slower!) spontaneous hydrolysis of phosphate triesters make available new data that complement previous work, by examining how reactivity depends on the non-leaving group (RO in Scheme 1).[11] The results suggested a subtle (but important) difference between the reactions of triaryl and dialkyl aryl triesters with the same leaving group, which can conveniently be examined by calculation and which can address detailed questions of mechanism and are not accessible to kinetic investigation. Recently we initiated a theoretical overview of structure−reactivity relationships in the spontaneous hydrolysis of phosphate triesters, specifically for the compounds **1a**, **1b**, **1d**, **2**, **3**, and **5** (Scheme 3).[19]

We present our detailed calculational examination of the mechanism of spontaneous hydrolysis for the series of triaryl and dialkyl aryl phosphate triesters shown in Scheme 3, using DFT.[20] The results include rate constants and thermodynamic parameters and define possible structural geometries for the rate-determining activated complexes.

■ COMPUTATIONAL METHODS AND MODELS

Quantum theoretical calculations for the hydrolysis reactions of triaryl (**1**, **2**) and tris-2-pyridyl (**3**) phosphates, together with dialkyl aryl phosphate triesters (**4**, **5**) shown in Scheme 3 were performed at the B3LYP and M06 levels of theory, with basic sets 6-31+G(d) and 6-311++G(d,p), using the GAUSSIAN 09 package implemented in Linux operating systems.[20] The default parameters for convergence, viz., the Berny analytical gradient optimization routine, were used: convergence on the density matrix was 10^{-9} atomic units, the threshold value for maximum displacement was 0.0018 Å, and the maximum force 0.00045 hartree/bohr. The energy minimum and the activated complex were identified in each case, and their structures characterized by frequency calculations at 1 atm and 298.15 K.[21] The frequency calculations give access to all thermodynamic quantities, such as zero-point vibrational energies (ZPVE), temperature corrections (E(T)), enthalpies, and free energies. Since solvent effects are important and can affect structure geometries significantly, all optimization and frequency calculation as well as other calculations were performed in the implicit presence of solvent using the default SCRF keyword and the polarizable continuum model (PCM) and the solvation model density (SMD).[22,23] Activated complexes (TS) were obtained by the quadratic synchronous transit (QST) protocol, and their structures identified by their single imaginary frequencies. Intrinsic reaction coordinates (IRC) were also computed to confirm the reaction paths.

The applicability of the implicit solvation model has been questioned, in the context of a mechanistic study of phosphate diester hydrolysis.[24] The appropriate model for a particular reaction must of course always be chosen with due care, but for calculations involving water as a reactant the combination of implicit and explicit solvation methodologies is both practical and appropriate since proton transfers are an integral part of the chemistry (in fact, an isolated water molecule is statistically insignificant).

dx.doi.org/10.1021/jo301380v | J. Org. Chem. 2012, 77, 7061−7070

To follow changes in charge distribution over the reaction, Hirshfeld and NBO charges[25−27] were calculated, while bond orders in activated complexes (**TS1**), reactants (**R**), and intermediates (**Int**) were compared using a natural population analysis (NPA) calculation as implemented in Gaussian 09.[28−31] Wiberg bond indices B_i can be used to estimate bond orders from population analysis, and the bond-breaking and making processes involved in the rate-limiting step were examined by means of the synchronicity (Sy) concept proposed by Moyano et al.[32] and described by eq 1:

$$Sy = 1 - [\sum_{i=1}^{n} |\delta B_i - \delta B_{av}|/\delta B_{av}]/2n - 2 \quad (1)$$

where n is the number of bonds directly involved in the activated complex, and the relative variation of the bond index is obtained from eq 2:

$$\delta B_i = [B_i^{TS} - B_i^{R}]/[B_i^{Int} - B_i^{R}] \quad (2)$$

where superscripts R, TS, and Int represent reactant, activated complex and intermediate, respectively. The evolution in bond order is calculated as $\%E_v = \delta B_i \times 100$, and its average value taken from eq 3:

$$\delta B_{av} = 1/n \sum_{i=1}^{n} \delta B_i \quad (3)$$

Wiberg Bond indices B_i were calculated for those bonds directly or indirectly involved in the hydrolysis process, namely, P_1-O_2, O_2-H_3, H_3-O_4, O_4-H_5, H_5-O_6, O_6-P_1, P_1-O_8, O_8-C_9, P_1-O_7, and O_6-H_{11} (For the atom numbering scheme see Scheme 4, below).

Scheme 4. TS1, Showing Atom Numbering Used for All Compounds

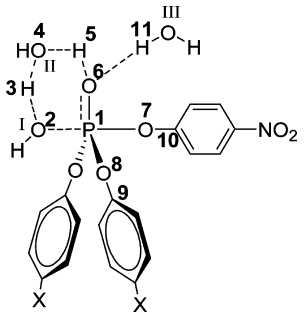

RESULTS AND DISCUSSION

Thermodynamic Parameters. We use DFT to evaluate potential energy surfaces (PES) for the hydrolysis reactions of all eight triesters (**1**−**5**) of Scheme 3. Stationary points are located to characterize reactant (**R**), activated complexes (**TS**), intermediates (**Int**), and products (**P**) and thus to obtain activation parameters. Initially, two possible mechanisms (mechanisms **1** and **2**) were considered (Figures 1 and 2). In both cases reaction involves attack of the oxygen atom of water on the central phosphorus atom. Mechanism **1** is a classical $S_N2(P)$ process, while mechanism **2** corresponds to a two-step addition−elimination pathway, via a pentacoordinated intermediate (**Int**). Table 1 compares calculated and experimentally observed parameters for the reaction of diphenyl 4-nitrophenyl phosphate (**1a**) with a single discrete water molecule.

The results in Table 1 show poor agreement between theoretical results and experiment, but $\Delta G^{\ddagger}$ for the two-step mechanism is closer by approximately 3 kcal/mol to the experimentally observed value.[11] So to investigate the specific effects of additional water molecules, we concentrated on two-step mechanisms. All attempts to calculate the classical $S_N2(P)$ mechanism**1** using two water molecules resulted in the formation of pentacovalent intermediates, as shown in mechanism **3** (Figure 3). Mechanism **3** is an extension of mechanism **2**, with an additional water molecule assisting the hydrolysis reaction by allowing two undemanding proton transfers, via a concerted six-membered cyclic activated complex (**TS1**) that includes general base catalysis in the first step and the cleavage of the pentacoordinated intermediate through **TS2** in the second step.

To evaluate the effect of the methodology used in the calculation, and to take into account non-covalent interactions, the calculations were performed using both hybrid density functionals B3LYP and M06, with basic sets 6-31+G(d) and 6-311++G(d,p).

The calculations for mechanism **3** give a free energy of activation significantly closer to the experimental value, and when a third water molecule is included in the calculation (Table 2), the free energy of activation agrees very closely with the experimental value in the B3LYP/6-31+G(d) level of theory, with less computational cost. Adding more than three water molecules gives almost the same value of the activation free energy (Table 2), so three discrete water molecules appear sufficient to describe the hydrolysis process in detail. The positioning of these molecules and the specific roles they play are based on many years of mechanistic work on this type of hydrolysis reaction. The activation free energy obtained by the recent meta-hybrid generalized gradient approximation (MHGGA) of M06[33] is in a reasonable agreement with the experimental values, although it underestimates the activation free energy by approximately 4 kcal/mol. The entropy of activation would also be expected to be highly negative, as indeed it is in the only available measurements of −35.6 eu for the hydrolysis of the 2,4-dinitrophenyl ester **2** and −36.2 eu for **TPP** hydrolysis.[19]

Interesting ab initio calculations for cyclic activated complexes involving water molecules have been reported for the hydration reactions of carbon dioxide, carbon disulfide, carbonyl sulfide, and carbodiimide at the MP2/aug-cc-pVTZ and Coupled-cluster theory (CCSD(T)) levels of theory.[34−37] The authors evaluated the possible participation of 1−4 water

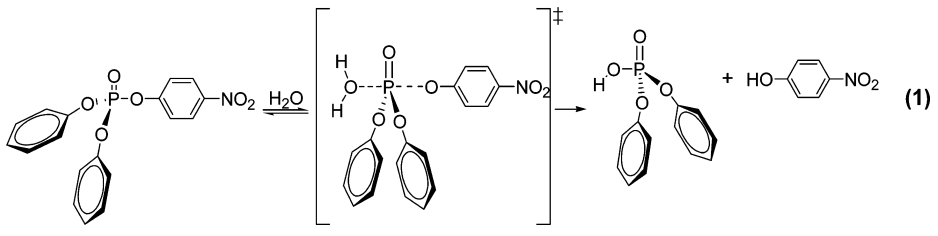

Figure 1. Mechanism **1**: the $S_N2(P)$ mechanism for hydrolysis using a single water molecule.

dx.doi.org/10.1021/jo301380v | J. Org. Chem. 2012, 77, 7061−7070

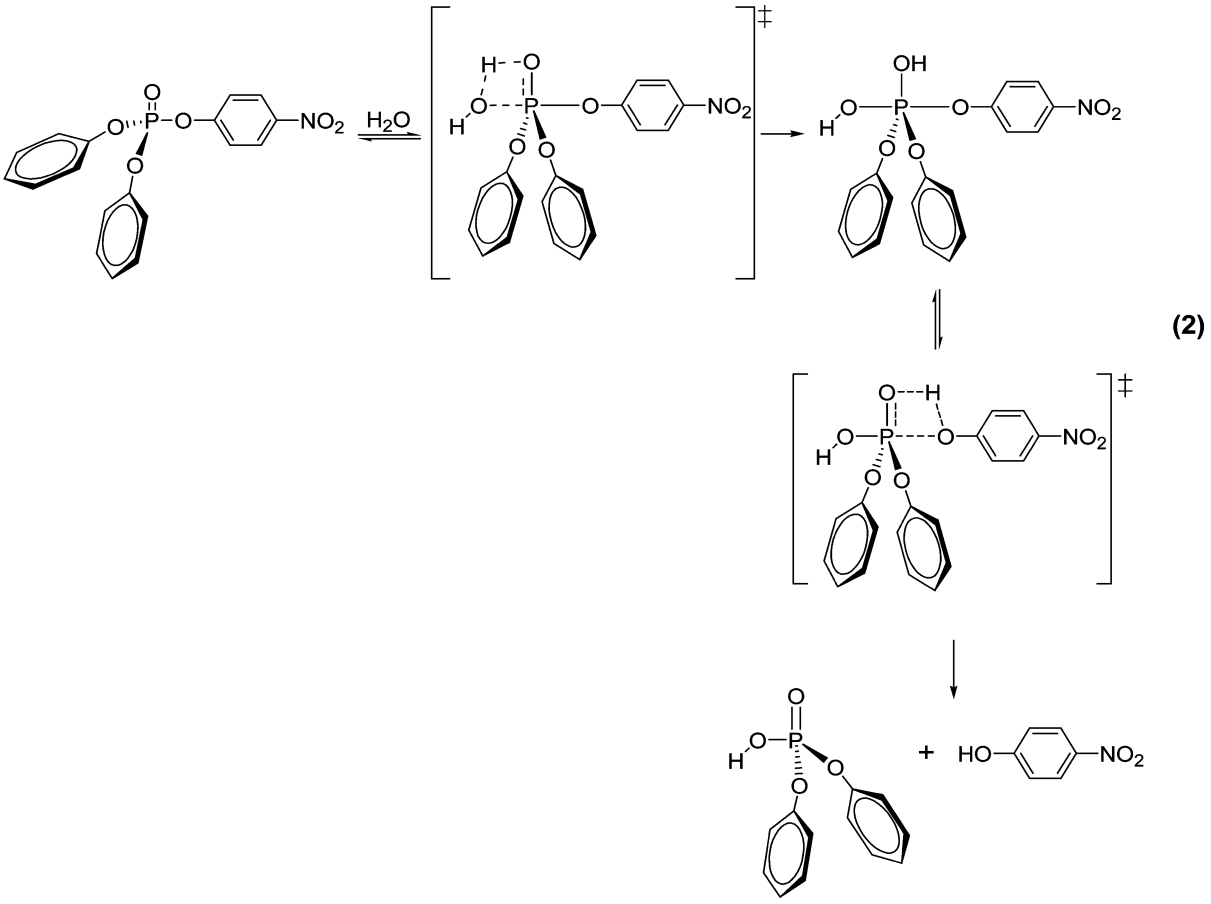

Figure 2. Mechanism **2**: the two-step mechanism for hydrolysis using a single water molecule.

Table 1. Activation Free Energies for the Hydrolysis of Diphenyl 4-Nitrophenyl Phosphate (1a) at 25 °C, Calculated at the B3LYP/6-31+g(d) Level of Theory with the PCM Solvation Model

mechanism	$\Delta G^{\ddagger}$(kcal/mol)
mechanism **1** (1 H_2O)	43.7
mechanism **2** (1 H_2O)	40.5
experimental[a]	24.8

[a]Experimental data taken from ref 11.

molecules in four-, six-, and eight-membered ring activated complexes. For the neutral hydration reaction of carbon dioxide two pathways were favored, one involving three water molecules directly in an eight-membered activated complex supporting 3 proton transfers and the second a six-membered ring activated complex with 2 water molecules supporting 2 proton transfers, with the third water molecule forming a separate hydrogen bond.[34] We examined a possible eight-membered ring activated complex involving 3 proton transfers in the hydrolysis reaction of diphenyl-4-nitrophenyl phosphate. Results obtained using three (**TS3**) and four (**TS4**) water molecules are shown in Figure 4 (Cartesian coordinates for the two activated complexes are included in the Supporting Information.

The activation free energies obtained for the two pathways are 20.5 and 21.1 kcal/mol for the **TS3** and **TS4**, respectively. The calculations for these eight-membered activated complexes underestimate the observed activation free energies by approximately 4 kcal/mol. The calculation for the six-membered ring activated complex (involving two proton transfers, with the third water molecule forming a stabilizing hydrogen bond) shows the best agreement with experiment. This result, involving two proton transfers, is consistent with the experimental (proton inventory and isotopic effect) evidence for the hydrolysis of tris-(2-pyridyl)phosphate (**3**).[11] The difference in geometry between the phosphate triesters and CO_2 can explain the difference between these substrates. In the phosphate triesters the angle ∠OPO is approximately 110°, and in the CO_2 the angle ∠OCO is 180°. Also, in the activated complexes for the hydration reactions the angle ∠OPO is approximately 90° compared with about 120° for ∠OCO. The greater angles are key to the explanation for the greater number of water molecules necessary to complete the more stable activated complex.

The activated complexes for the rate-determining formation (**TS1**) and cleavage (**TS2**) of the pentacoordinated intermediate were verified by means of IRC calculations for the hydrolysis of **1a** in the presence of three water molecules (Figure 5). The IRC shows an unstable intermediate (calculated half-life less than a millisecond), with water molecules playing well-defined roles in its formation and cleavage. Two water molecules are directly involved in bond making and breaking in the rate-determining activated complex, supporting the two proton transfers, while the third is hydrogen-bonded to P═O_6. This result, with two proton transfers, is consistent with the experimental evidence reported in the literature for the hydrolysis of tris-(2-pyridyl)phosphate (**3**).[11] The third water molecule is also involved in the cleavage of the intermediate, as discussed below. Figure 6 shows

dx.doi.org/10.1021/jo301380v | J. Org. Chem. 2012, 77, 7061−7070

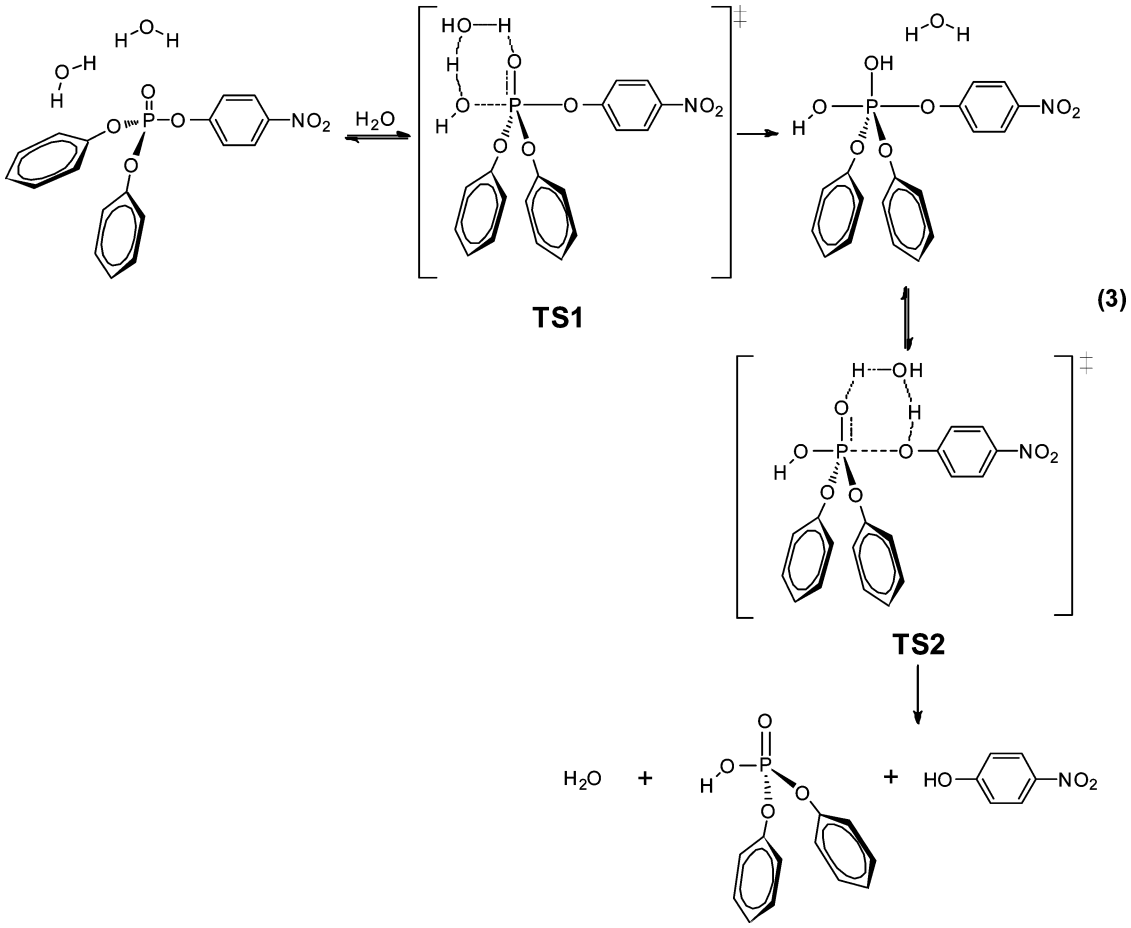

Figure 3. Mechanism **3**: the two-step mechanism for hydrolysis using two discrete water molecules.

Table 2. Activation Free Energies (kcal/mol) for the Hydrolysis of Diphenyl 4-Nitrophenyl Phosphate (1a): Calculated for Mechanism 3 at 25 °C with 1, 2, 3, and 4 Discrete Water Molecules Present, at Different Levels of Theory with the PCM Solvation Model

	B3LYP		M06	
mechanism	6-31+G(d)	6-311++G(d,p)	6-31+G(d)	6-311++G(d,p)
mechanism **2** (1 H_2O)	40.5	40.4	35.2	37.6
mechanism **3** (2 H_2O)	27.8	26.3	20.3	21.7
mechanism **3** (3 H_2O)	25.2	25.1	20.2	19.8
mechanism **3** (4 H_2O)	25.4	26.5	18.8	20.7
experimental[a]	24.8			

[a]Experimental data taken from ref 11.

optimized structures for **TS1** and **TS2**, for the hydrolysis reaction of **1a**. IRCs for all other compounds (**1b**–**5**) are shown in Figure S2 of the Supporting Information.

Using the model activated complex **TS1** of Figure 6, similar theoretical calculations were performed for all eight triesters shown in Scheme 2. Results are summarized in Table 3. There is good agreement between calculated and experimental free energies of activation (mean difference 0.05 ± 0.41 kcal/mol) over the series. The results show a dependence of reactivity on both leaving and non-leaving groups, as recently found experimentally.[11]

Where the non-leaving groups are the same (e.g., **2** vs **3**), we find that reactivity depends, as expected, on the leaving group (the pK_a of *p*-nitrophenol is lower than that of 2-hydroxypyridine), but reactivity also varies over a wide range for systems with the same (*p*-nitrophenol) leaving group when the non-leaving groups are varied, over the series **1d** > **2** > **1c** > **1b** > **1a** > **4** > **5**. Increasing the electron-withdrawing ability of the two non-leaving groups can accelerate the reaction by many orders of magnitude. The good agreement shown in Table 3 between calculated and theoretical values confirms that the two so-called "spectator" *p*-nitrophenoxy groups of **1d** have significant effects, when compared with the two MeO groups of dimethyl *p*-nitrophenyl phosphate, the least reactive triester studied. The two pNPO groups increase the electrophilicity of the phosphorus center of the reactant and stabilize both activated complex and pentacovalent intermediate. The structure of the TS and changes in geometrical parameters, charges, and bond orders are described in detail in the following sections.

Activated Complex and Mechanism. Scheme 4 shows the atom numbering system used for the activated complex **TS1** of Figure 5. Scheme 4 indicates the bonds being made or broken, namely, the formation of P_1–O_2 with concomitant transfers of H_3 (cleavage of O_2–$H_3$and formation of H_3–O_4) and H_5 (cleavage of O_4–H_5 and formation of H_5–O_6), in the general base-catalyzed attack of water oxygen on phosphorus. Table S1 in the Supporting Information gives relevant

dx.doi.org/10.1021/jo301380v | J. Org. Chem. 2012, 77, 7061–7070

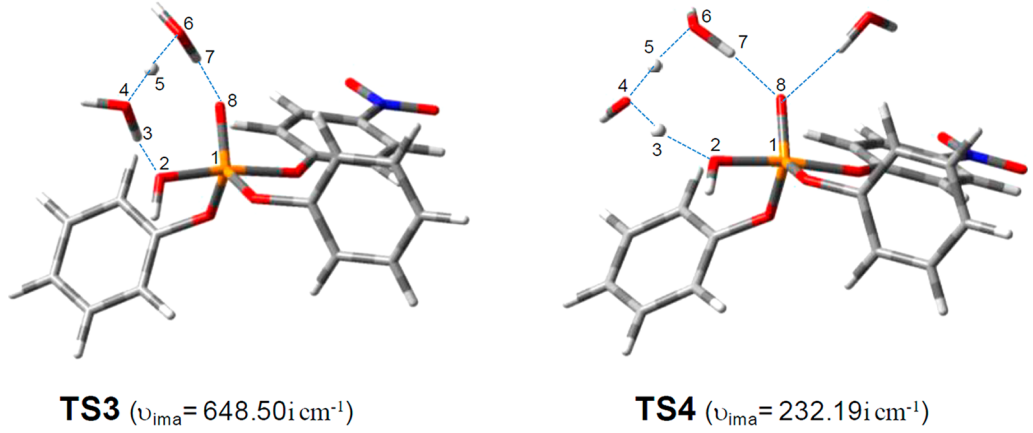

Figure 4. Eight-membered activated complexes with three (**TS3**) and four (**TS4**) water molecules involved in the hydrolysis reaction of diphenyl-4-nitrophenyl phosphate (**1a**).

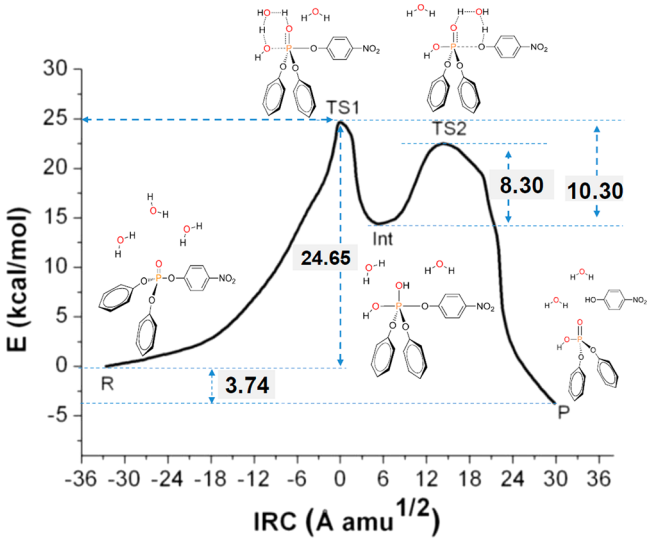

Figure 5. Intrinsic reaction coordinate for the hydrolysis of diphenyl 4-nitrophenyl phosphate (**1a**), calculated for mechanism **3** [3 H_2O], using a step size of 0.1 bohr $amu^{0.5}$.

Table 3. Activation Free Energy and Rate Constant of Hydrolysis of Triaryl Triesters (1 and 2), Tris-2-pyridyl phosphate (3), and Dialkyl Aryl Phosphate Triesters (4 and 5) with 3 Water Molecules at 25 °C at the B3LYP/6-31+g(d) Level of Theory with the PCM Solvation Model

	experimental[a]	calculated
compd	$\Delta G^{\ddagger}$ (kcal/mol)	$\Delta G^{\ddagger}$ (kcal/mol)
1a	24.8	25.2
1b	24.0	24.7
1c	23.6	23.5
1d	21.9	22.3
2	23.4	23.8
3	24.5	25.5
4	24.8	26.2
5	29.6	30.0

[a]Experimental data taken from ref 11.

structural parameters calculated for the reactant (**R**), rate-determining activated complex (**TS1**), and intermediate (**Int**) formed in the rate-determining step for all eight compounds of Scheme 3.

A major decrease in the interatomic distance P_1-O_2 is observed on going from the reactant to **TS1**: from 4.85 Å to 1.78 Å for **1a**, and from 5.25 Å to 1.79 Å for **1c**. The distance P_1-O_2, between the approaching nucleophilic water molecule and triester P, differs from substrate to substrate, but in the activated complex P_1-O_2 is practically the same, at ca. 1.8 Å. A

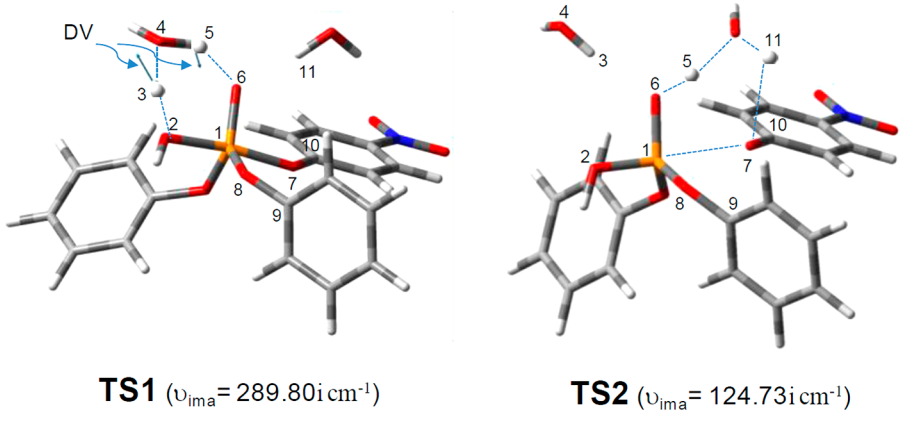

Figure 6. Optimized structures of **TS1** and **TS2** for the hydrolysis reaction of **1a**. Cartesian coordinates for all compounds are given in the Supporting Information. DV refers to the displacement vectors for H_3 transfer from O_2 to O_4 and for H_5 transfer from O_4 to O_6.

dx.doi.org/10.1021/jo301380v | J. Org. Chem. 2012, 77, 7061−7070

significant corresponding increase in the O_2-H_3 distance from 0.98 to 0.99 Å to 1.39−1.41 Å is also found for all compounds, as is the concurrent decrease in the H_3-O_4 distance, from 1.82 to 1.90 Å to 1.09−1.10 Å. However, the O_4-H_5 distance does not change significantly from reactant to activated complex. The H_5-O_6 distance decreases from reactant to **TS1** because H_5, only hydrogen-bonded to the phosphoryl oxygen in the reactant, is beginning to be transferred to it in the activated complex.

The dihedral angles (Table S1 in the Supporting Information) are consistent in all cases with a nonplanar six-membered cyclic activated complex $P_1-O_2-H_3-O_4-H_5-O_6$, with imaginary frequencies between 162 and 313 cm^{-1}. These correspond to the rocking vibration leading to intermediate formation. The displacement vectors (DV) associated with the imaginary frequency show that two significant proton transfers (H_3 moving in the direction of O_4 and H_5 in the direction of O_6) play crucial roles in the stabilization of **TS1**. The vectors describing these H_3 and H_5 movements are included in Figure 6 to indicate the physical nature of the effect. The resultant conversion of P═O from double to partial single bond is clearly marked by the increase in the O_6-P_1 distance. In the activated complex O_6 is also hydrogen-bonding to H_{11} (of the third water molecule), as indicated by the decrease in the distance O_6-H_{11} from 1.90−1.92 Å to 1.80−1.82 Å. This hydrogen-bonding plays a significant role in stabilizing the developing atomic charge on O_6 in the activated complex.

The most detailed information about bond making and breaking at P comes from the variation of P−O bond lengths as reaction proceeds and especially in the activated complex (Table 4). Figure 7 shows how these bond lengths for four

Table 4. Interatomic Distances (Å) for the Activated Complex (TS1) for All Eight Compounds Calculated at the B3LYP/6-31+g(d) Level of Theory[a]

	1a	1b	1c	1d	2	3	4	5
O_2-P	1.78	1.78	1.78	1.78	1.79	1.80	1.79	1.80
$P-O_6$	1.54	1.54	1.53	1.5,	1.53	1.54	1.54	1.55
$P-O_7$	1.77	1.77	1.77	1.76	1.77	1.74	1.77	1.79
$P-O_8$	1.65	1.65	1.65	1.66	1.65	1.80	1.65	1.63

[a]Complete results are shown in Table S2 of the Supporting Information.

representative *p*-nitrophenyl triesters depend on the nature, specifically, the pK_a, of the non-leaving groups. As expected, at the TS "balance point", the lengths of the two axial bonds to the oxygen atoms of the entering and leaving groups are almost identical for each compound and significantly longer than those to the oxygens in the equatorial plane of the trigonal bipyramid. Of these the bond to the phosphoryl oxygen retains some double bond character so is naturally the shortest. However, all three show negative slopes in the plot of Figure 7; these are similar for the two apical groups but significantly smaller for $P{=}O_6$ (1.7×10^{-3} vs 3.3×10^{-3} for $P-O_2$ and $P-O_7$). Thus increasing electron withdrawal by the two non-leaving groups stabilizes the **TS** in terms of shorter bonds to the other oxygens but has the expected lengthening effect on $P-O_8$, defining a bond length correlation of negative slope (-0.29×10^{-3}), opposite in sign but comparable in magnitude with those of the two bonds being made and broken. This comparison makes very clear how triester reactivity in these and related systems depends more or less equally on all four activated complex

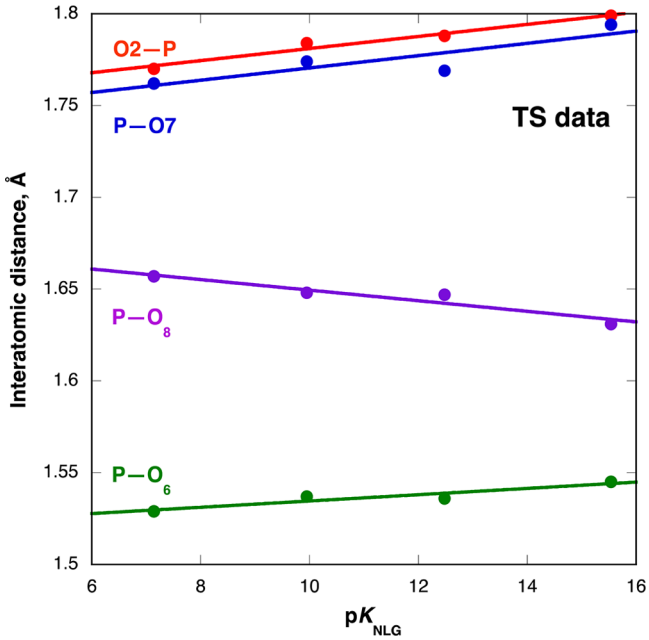

Figure 7. Dependence of bond lengths P−O at the phosphorus center in the activated complex (**TS1**) on the pK_a of the non-leaving group ROH, for four *p*-nitrophenyl esters $(RO)_2P(O)-OpNP$ (**1a**, **1d**, **4**, and **5**). Activated complex bond orders (see Figure 9, below, and data in Table S3 in the Supporting Information) show commensurate changes over the series.

ligands: nucleophile, leaving group, and the two non-leaving groups.

Charge Distribution. To describe the changes in charge distribution occurring as the reaction proceeds, we calculated Hirshfeld and NBO charges for the atoms involved directly in the formation of the activated complex, namely, P_1, O_2, H_3, O_4, H_5, O_6, O_7, and O_8 (Supplementary Tables S2 and S3, respectively). These atoms show only minor changes in charge distribution from one compound to another, because the chemical environments are closely similar. In the NBO charges the phosphorus center carries a substantial positive charge of approximately 2.6, which is reduced by only some 2% in the activated complex as also is the negative charge on the oxygen O_2 of the attacking water (from about −1.08 to −1.06). Significant charge development, as high as 12%, is most apparent in the two solvent water molecules involved in general base catalysis, rather than on the nucleophile or leaving group oxygens. The instructive conclusion is that the catalyst and the solvent (in this case the same thing) make the main contribution to stabilizing developing charge in the activated complex. No correlation between the NBO charges and the pK_{NLG} was found over the series.

For the Hirshfeld charges, the phosphorus center carries a significant positive charge of 0.6−0.7, which is reduced by some 10% in the activated complex (where it mirrors reactivity, with a linear dependence on pK_{NLG} (Supplementary Figure S1). Major changes on forming the activated complex are observed, as expected, in the atomic charges on the oxygens of the attacking water and the leaving group (O_2 and O_7, which undergo average changes of +45% and −27%, respectively). In addition, the phosphoryl $P{=}O_6$ and non-leaving group oxygens O_8 together accommodate as much of the developing negative charge as the leaving group. However, the maximum charge development, change as high as +69%, occurs in the

dx.doi.org/10.1021/jo301380v | J. Org. Chem. 2012, 77, 7061−7070

second water molecule, involved as a general base (Figure 8). As found above, the instructive conclusion is that the catalyst

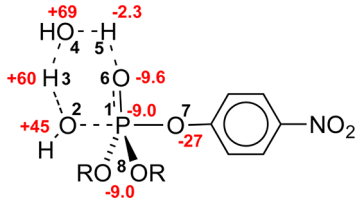

Figure 8. Percentage changes in atomic charges in **TS1** relative to reactant (averaged over the 8 triesters). Data from Table S2 in the Supporting Information.

and the solvent make the main contribution to stabilizing charge development in the activated complex. We consider that Hirshfeld charges describe the hydrolysis process of phosphate triesters more accurately.

Bond Order Analysis. Bond order calculations were performed using Gaussian 09.[19] Wiberg bond indices are estimated from natural population analysis (NPA). Bond-breaking and making processes involved in the rate-limiting step were examined by means of the synchronicity (Sy) concept proposed by Moyano et al. The resulting indices are shown in Table S4 in the Supporting Information. Wiberg bond indices B_i were calculated for all of the bonds changed in the hydrolysis reaction, as shown in Scheme 3, namely, P_1-O_2, O_2-H_3, H_3-O_4, O_4-H_5, H_5-O_6, O_6-P_1, P_1-O_8, O_8-C_9, P_1-O_7, and O_6-H_{11}. Other bonds undergo negligible changes and are not considered.

The estimated bond orders P_1-O_2, O_2-H_3, H_3-O_4, O_4-H_5, H_5-O_6, O_6-P_1 for bond making and breaking in **TS1** (Table S4 in the Supporting Information) indicate that P_1-O_2 bond formation is most advanced (mean $\%E_v$ = 77.83 ± 0.97%), followed by O_2-H_3 cleavage (mean $\%E_v$ 69.80 ± 2.25) and the formation of H_3-O_4 (mean $\%E_v$ 63.11 ± 2.38), the two proton transfers integral to general base catalysis. The concurrent development of O_2-H_3 and H_3-O_4 shows clearly how these two water molecules participate directly in the formation of the activated complex. The third water molecule is involved in a hydrogen bond, which becomes stronger in the activated complex for **1a**, **3**, and **5** (Wiberg index increasing from ~0.0005 in the reactant to ~0.05 in the activated complex), thus stabilizing the developing charge on O_6. However, in compounds **1b–d**, **2**, and **4** this hydrogen bond scarcely changes from reactant to activated complex **TS1** (~0.03 for the reactant and ~0.05 for the activated complex). The average degree of evolution of bond order (% δB_{av}) is less than 50%, suggestive of a relatively early activated complex with associative character.

As a measure of the concertedness of the reaction the synchronicity parameter Sy was used. Note that this study is concerned specifically with bond- making and partial bond breaking in the (primarily, see below) rate-determining **TS1**, i.e., the bonds P_1-O_2, O_2-H_3, H_3-O_4, O_4-H_5, H_5-O_6, O_6-P_1, which define the six-membered cyclic activated complex involved in the formation of the intermediate. The departure of the leaving group it is not taken into account in this analysis. The synchronicity parameter varies from zero, in the case of an asynchronous process, to unity for a concerted synchronous reaction. In a multicentered process the reaction can be further advanced in some reaction coordinates than others. In this reaction the rate-determining step is **TS1**, involving the attack of the water on the phosphorus atom and its supporting proton transfers. Taking the intermediate formation reaction as a single process, the reactions show a considerable degree of asynchronicity, $0.655 \leq Sy \leq 0.697$ (Table S4 in the Supporting Information).

To further confirm the importance of the non-leaving group in the hydrolysis process we present one more correlation (of many), between the Wiberg bond indices for all of the P–O bonds involved in the activated complex TS1 with the pK_a values of the non-leaving groups (Table 5, Figure 9). Satisfactory correlations are observed, mirroring the bond-length correlations of Figure 7 (higher bond order corresponding to shorter bond).

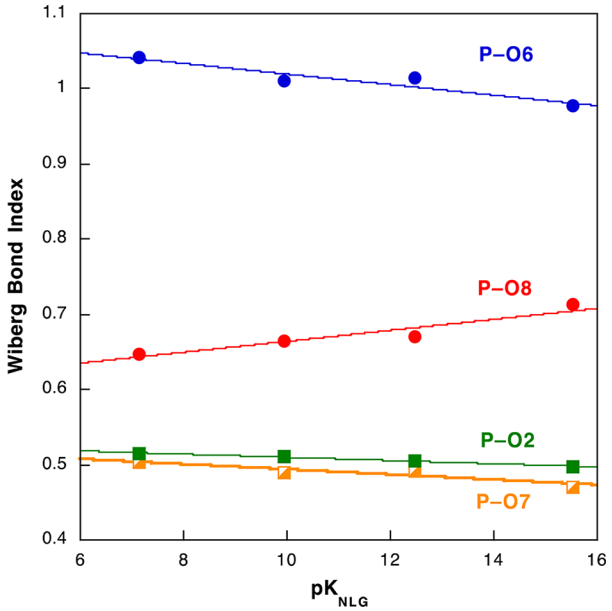

Figure 9. Activated complex Wiberg bond index-reactivity correlations with non-leaving group pK_a values for compounds **1a**, **1d**, **4**, and **5**. Data from Table S3 of the Supporting Information.

Kinetic Significance of TS2. Kinetic measurements provide no information about steps in a reaction that are not

Table 5. Wiberg Bond Indices for the Activated Complex (TS1) for All Eight Compounds, Calculated at the B3LYP/6-31+g(d) Level of Theory[a]

	1a	1b	1c	1d	2	3	4	5
O_2-P	0.511	0.515	0.512	0.515	0.509	0.502	0.505	0.498
$P-O_6$	1.010	1.016	1.022	1.043	1.030	1.008	1.014	0.977
$P-O_7$	0.490	0.493	0.493	0.503	0.497	0.526	0.492	0.471
$P-O_8$	0.664	0.662	0.661	0.648	0.656	0.648	0.670	0.712

[a]Complete results are shown in Table S4 of the Supporting Information.

dx.doi.org/10.1021/jo301380v | J. Org. Chem. 2012, 77, 7061–7070

Table 6. Comparison of Forward and Reverse Reactions of INT for *p*-Nitrophenyl Esters

	$\Delta G^{\ddagger}$ (kcal mol^{-1})		derived rate constants and ratios		
compd	**TS1** (reverse)	**TS2** (forward)	$10^{-3} \times k_{-1}/k_2$	$10^{-6} \times k_{obs}$ (s^{-1})	$10^{-6} \times k_1$ (s^{-1})
1a	10.3	8.1	23.4	3.78	3.87
1b	9.2	7.2	32.2	15.4	15.9
1c	9.4	8.1	119.1	28.7	32.1
1d	9.2	9.1	913.6	541.0	1040.0
2	10.8	9.0	49.4	46.8	49.1
4	11.6	7.2	0.5	4.41	4.41
5	11.3	3.3	1.0×10^{-3}	1.27×10^{-3}	1.27×10^{-3}

rate-determining, but the quantitative data available from the calculations, displayed in the IRCs of Figure 5 and Supplementary Figure S2, allow direct comparison of the forward and reverse reactions of the pentacovalent intermediate in each case. We performed frequency calculations for reactant, activated complexes **TS1** and **TS2**, and intermediate (**Int**) in order to obtain free energies for each stationary point. The data are compared in Table 6, and the rate constants and their relationships are defined in Scheme 5.

Scheme 5. Rate Constants and Ratios for the Formation and Breakdown of the Pentacovalent Addition Intermediate Int (Figure 5)

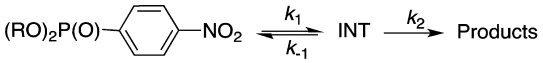

$$k_{obs} = \frac{k_1 k_2}{k_{-1} + k_2} \quad \text{so} \quad k_1/k_{obs} = 1 + k_{-1}/k_2$$

Using the Eyring equation for the classical activated complex theory (TST) $k_{obs} = (k_B T/h)\, e^{-\Delta G^{\ddagger}/RT}$ to compare the forward and reverse reactions of **Int** (Figure 5) gives the expression $\ln(k_{-1}/k_2) = (\Delta G^{\ddagger}(2) - \Delta G^{\ddagger}(-1))/RT$, from which we can derive the rate constants and ratios shown in Table 6. The ratios show that **TS1** is cleanly rate-determining for the dimethyl triester **5** but becomes only partially rate-determining for the most reactive systems, with the most electron-withdrawing non-leaving groups; thus for tris-4-nitrophenyl phosphate **1d** k_{obs} is some 30% slower than expected if **TS1** is the only barrier. Plotting the calculated $\Delta G^{\ddagger}$ against pK_{NLG} (Figure 10) shows that the dependence on the non-leaving group is significantly greater for the breakdown of **Int**, which is predicted to become the principal barrier to reaction for compounds with more electron-withdrawing non-leaving groups than **1d**. The small dependence for the reverse reaction (k_{-1}) is consistent with the early activated complex for the breakdown of a high energy species, and the minimal charge changes on P and on O8 involved in the formation of the intermediate (Figure 10 and Table 6).

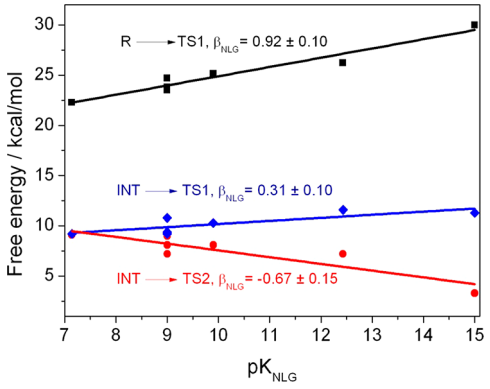

Figure 10. Dependence on the non-leaving group of $\Delta G^{\ddagger}$ compared for formation of intermediate Int (diamonds) and its breakdown to reactants and product. Data from Table 6.

CONCLUSION

This work presents detailed evidence about the mechanism of spontaneous hydrolysis of phosphate triesters, calculated for the reactions of selected triesters with common leaving groups and varying non-leaving groups. Where direct comparisons are possible the calculations are in good agreement with available experimental data. General base catalysis supports the rate-determining formation of the new P–O bond by way of a six-membered cyclic activated complex **TS1**, with a mean percentage evolution ($\%E_v$) = 77.83 ± 0.97%. A third water molecule stabilizes the activated complex by way of a developing hydrogen bond (the Wiberg bond index increasing to 0.0492 in **TS1** from almost zero in the reactant for **1a**). Reaction clearly involves a two-step pathway, with a pentacovalent intermediate on the reaction coordinate, as illustrated by the IRC depicted in Figure 5. Formation of the new P_1–O_2 bond is over 77% complete in the rate-determining step in all cases. Finally, this work corroborates and supports the significant role played by the non-leaving groups in the hydrolysis of phosphate triesters, in the shape of well-defined correlations between bond lengths and Wiberg bond indices with the pK_a's of the non-leaving groups, and defines specific roles for the water molecules directly involved in general base catalysis of the spontaneous hydrolysis reaction.

ASSOCIATED CONTENT

Supporting Information

Cartesian coordinates for reactant (**R**), activated complex (**TS1**), and intermediate (**INT**) for all compounds considered in this article. Geometrical Parameters, Hirshfeld and NBO charges, and Wiberg bond indices for all structures, and complete IRCs for the stepwise hydrolysis reaction for all compounds. This material is available free of charge via the Internet at http://pubs.acs.org.

AUTHOR INFORMATION

Corresponding Author

*E-mail: faruk.nome@ufsc.br; ajk1@cam.ac.uk.

Notes

The authors declare no competing financial interest.

dx.doi.org/10.1021/jo301380v | J. Org. Chem. 2012, 77, 7061–7070

■ ACKNOWLEDGMENTS

We are grateful to INCT-Catálise, FAPESC, CNPq and CAPES for support of this work.

■ REFERENCES

(1) Cleland, W. W.; Hengge, A. C. *Chem. Rev.* **2006**, *106*, 3252.
(2) Hengge, A. C. In *Advances in Physical Organic Chemistry*; Richard, J. P., Ed.; Academic: New York, 2005; Vol. *40*, p 49.
(3) Lassila, J. K.; Zalatan, J. G.; Herschlag, D. *Annu. Rev. Biochem.* **2011**, *80*, 669.
(4) Raushel, F. M.; Holden, H. M. *Adv. Enzymol. Ramb.* **2000**, *74*, 51.
(5) Brown, R. S.; Neverov, A. A. In *Advances in Physical Organic Chemistry*; Richard, J. P., Ed.; Academic: New York, 2008; Vol. *42*, p 271
(6) Ugwumba, I. N.; Ozawa, K.; Xu, Z.-Q.; Ely, F.; Foo, J.-L.; Herlt, A. J.; Coppin, C.; Brown, S.; Taylor, M. C.; Ollis, D. L.; Mander, L. N.; Schenk, G.; Dixon, N. E.; Otting, G.; Oakeshott, J. G.; Jackson, C. J. *J. Am. Chem. Soc.* **2011**, *133*, 326.
(7) Smith, B. M. *Chem. Soc. Rev.* **2008**, *37*, 470.
(8) Kim, K.; Tsay, O. G.; Atwood, D. A.; Churchill, D. G. *Chem. Rev.* **2011**, *111*, 5345.
(9) Kirby, A. J.; Tondo, D. W.; Medeiros, M.; Souza, B. S.; Priebe, J. P.; Lima, M. F.; Nome, F. *J. Am. Chem. Soc.* **2009**, *131*, 2023.
(10) Khan, S. A.; Kirby, A. J. *J. Chem. Soc. B* **1970**, 1172.
(11) Kirby, A. J.; Medeiros, M.; Oliveira, P. S. M.; Orth, E. S.; Brandão, T. A. S.; Wanderlind, E. H.; Amer, A.; Williams, N. H.; Nome, F. *Chem.—Eur. J.* **2011**, *17*, 14996.
(12) Kamerlin, S. C. L.; Wilkie, J. *Org. Biomol. Chem.* **2011**, *9*, 5394.
(13) Yang, Y.; Yu, H.; York, D.; Elstner, M.; Cui, Q. *J. Chem. Theory Comput.* **2008**, *4*, 2067.
(14) Kamerlin, S. C. L.; Florian, J.; Warshel, A. *ChemPhysChem* **2008**, *9*, 1767.
(15) Klaehn, M.; Rosta, E.; Warshel, A. *J. Am. Chem. Soc.* **2006**, *128*, 15310.
(16) Zhang, X.; Wu, R.; Song, L.; Lin, Y.; Lin, M.; Cao, Z.; Wu, W.; Mo, Y. *J. Comput. Chem.* **2009**, *30*, 2388.
(17) Chen, S.-L.; Fang, W.-H.; Himo, F. *J. Phys. Chem. B* **2007**, *111*, 1253.
(18) Tarrat, N. *J. Mol. Struct. THEOCHEM* **2010**, *941*, 56.
(19) Mora, J. R.; Kirby, A. J.; Nome, F. *Biochim. Biophys. Acta* **2012**, in press; DOI:10.1016/j.bbapap.2012.04.010.
(20) Frisch, M. J.; Trucks, G. W.; Schlegel, H. B.; Scuseria, G. E.; Robb, M. A.; Cheeseman, J. R.; Scalmani, G.; Barone, V.; Mennucci, B.; Petersson, G. A.; Nakatsuji, H.; Caricato, M.; Li, X.; Hratchian, H. P.; Izmaylov, A. F.; Bloino, J.; Zheng, G.; Sonnenberg, J. L.; Hada, M.; Ehara, M.; Toyota, K.; Fukuda, R.; Hasegawa, J.; Ishida, M.; Nakajima, T.; Honda, Y.; Kitao, O.; Nakai, H.; Vreven, T.; Montgomery, J. A.; Jr.; Peralta, J. E.; Ogliaro, F.; Bearpark, M.; Heyd, J. J.; Brothers, E.; Kudin, K. N.; Staroverov, V. N.; Kobayashi, R.; Normand, J.; Raghavachari, K.; Rendell, A.; Burant, J. C.; Iyengar, S. S.; Tomasi, J.; Cossi, M.; Rega, N.; Millam, J. M.; Klene, M.; Knox, J. E.; Cross, J. B.; Bakken, V.; Adamo, C.; Jaramillo, J.; Gomperts, R.; Stratmann, R. E.; Yazyev, O.; Austin, A. J.; Cammi, R.; Pomelli, C.; Ochterski, J. W.; Martin, R. L.; Morokuma, K.; Zakrzewski, V. G.; Voth, G. A.; Salvador, P.; Dannenberg, J. J.; Dapprich, S.; Daniels, A. D.; Farkas, O.; Foresman, J. B.; Ortiz, J. V.; Cioslowski, J.; Fox, D. J. *Gaussian 09, Revision A.02.*; Gaussian, Inc., Wallingford, CT, 2009.
(21) McQuarrie, D. A. *Statistical Mechanics*; Harper & Row, 1976.
(22) Marenich, A. V.; Cramer, C. J.; Truhlar, D. G. *J. Phys. Chem. B* **2009**, *113*, 4538.
(23) Marenich, A. V.; Cramer, C. J.; Truhlar, D. G. *J. Phys. Chem. B* **2009**, *113*, 6378.
(24) Kamerlin, S. C. L; Haranczyk, M.; Warshel, A. *ChemPhysChem* **2009**, *10*, 1125.
(25) Hirshfeld, F. L. *Theor. Chim. Acta* **1977**, *44*, 129.
(26) Van Damme, S.; Bultinck, P.; Fias, S. *J. Chem. Theory Comput.* **2009**, *5*, 334.
(27) Guerra, C. F.; Handgraaf, J. W.; Baerends, E. J.; Bickelhaupt, F. M. *J. Comput. Chem.* **2004**, *25*, 189.
(28) Lendvay, G. *J. Phys. Chem.* **1989**, *93*, 4422.
(29) Reed, A. E.; Weinstock, R. B.; Weinhold, F. *J. Chem. Phys.* **1985**, *83*, 735.
(30) Reed, A. E.; Curtiss, L. A.; Weinhold, F. *Chem. Rev.* **1988**, *88*, 899.
(31) Wiberg, K. B. *Tetrahedron* **1968**, *24*, 1083.
(32) Moyano, A.; Pericas, M. A.; Valenti, E. *J. Org. Chem.* **1989**, *54*, 573.
(33) (a) Zhao, Y.; Truhlar, D. G. *J. Chem. Phys.* **2006**, *125* (1), 194101. (b) Zhao, Y.; Truhlar, D. G. *Theor. Chem. Acc.* **2008**, *120*, 215.
(34) Nguyen, M. T.; Matus, M. H.; Jackson, V. E.; Ngan, V. T.; Rustad, J. R.; Dixon, D. A. *J. Phys. Chem. A* **2008**, *112*, 10386.
(35) Deng, C.; Li, Q. G.; Ren, Y.; Wong, N. B.; Chu, S. Y.; Zhu, H. J. *J. Comput. Chem.* **2008**, *29*, 466.
(36) Deng, C.; Wu, X. P.; Sun, X. M.; Ren, Y.; Sheng, Y. H. *J. Comput. Chem.* **2009**, *30*, 285.
(37) Sun, X. M.; Wei, X. G.; Wu, X. P.; Ren, Y.; Wong, N. B.; Li, W. K. *J. Phys. Chem. A* **2010**, *114*, 595.